7th International Conference on Multiphase Flow,
ICMF 2010, Tampa, FL, May 30 – June 4, 2010

Air entrapment and splashing treshold in drop impacts.

C. Josserand, P. Ray and S. Zaleski

Institut D'Alembert, UMR 7190, CNRS & UPMC, Paris, France

christophe.josserand@upmc.fr

Keywords: drop impact, splash, jets

Abstract

We investigate here how the surrounding gas influence the dynamics of drop impacts on a thin liquid film. We describe in details the entrapment of the gas bubble using numerical simulations with high enough mesh resolution. The bubble entrapment comes from viscous effect in the thin gas layer that need to be evacuated down the drop, creating a high pressure field that deforms the drop interface into a dimple. We finally investigate how this dynamics coupling gas and liquid dynamics can change the splashing dynamics.

1 Introduction

Drop impact is a common mechanism in processes involving interface dynamicsRein (1993). Rain, atomization of liquid jets, ink-jet printing, stalagmite growth are typical examples where the impact of drops plays a crucial role. Depending on the context, the drop can impact on a dry surface, a thin liquid film or a deep liquid bath. Always, the drop deforms under the impact and it can lead to very different outcomes (Coantic (1980); Prosperetti and guz (1993); Yarin and Weiss (1995); Josserand and Zaleski (2003); Renardy et al. (2003); Clanet et al. (2004); Josserand et al. (2005); Bartolo et al. (2005, 2006); Schroll et al. (2010)): spreading, prompt and/or corolla splashing, cavity formation for instance. The detail control of this output is complex since it is influenced by different physical balances such as inertia, capillary forces or viscous dissipation or also by geometrical considerations such as aspect ratios or surface roughness.

In this paper we investigate the influence of the surrounding fluid, often neglected in the litterature. Indeed, since the surrounding fluid is a gas in general, most often the air, its density is usually about one thousand time smaller than that of the liquid. Therefore its inertia will be much smaller than the liquid one and it is tempting to neglect the gas dynamics in the impact process. In fact, if this approximation is correct for the corolla dynamics or the late time spreading of the drop impact for instance, it is wrong at the short time scale around the onset of impact, because of the gas viscosity. As the drop approaches the impacting surface, the surrounding fluid has to be evacuated from the interstitial region. Under this cushioning, the lubrication effect due to viscous forces in the gas deforms the interfaces (of the drop and of the liquid film/bath if any) before the impact. One the most striking consequence of this viscous cushioning is that a bubble of gas can be entrapped either between the two liquid interface or between the drop and the substrate (guz and Prosperetti (1990); Mehdi-Nejad et al. (2003); Thoroddsen et al. (2003, 2005); Korobkin et al. (2008); Mandre et al. (2009)). Indeed, the lubrication of the thin gas layer creates a high pressure in the gas down the drop center. Such dynamics is illustrated on figure 1 where snapshots of the impact of a water drop on a thin liquid film surrounded by air obtained by numerical simulation (details given below) are shown.

Although the bubble entrapment in drop impact has been already mentioned in different experimental and numerical works, it has not been studied in details until recently for various reasons. Firstly, if the gas was clearly identified to play a role in the short time dynamics, it was also believed that it was not influencing the later dynamics of the impact. Therefore the air dynamics was often neglected or even not considered in analytical or numerical models. Moreover, "technical" reasons made this regime hard to investigate and characterize both experimentally and numerically: for instance the entrapped bubble is hard to see in experiments because of the light refraction at the interface. In the numerics the surrounding fluid was often neglected either by sake of simplicity or because the mesh size available could not allow a consistent resolution of the gas cushioning so that the numerical simulations were avoiding in purpose a detailed account of this regime (see Josserand and Zaleski (2003) for instance).

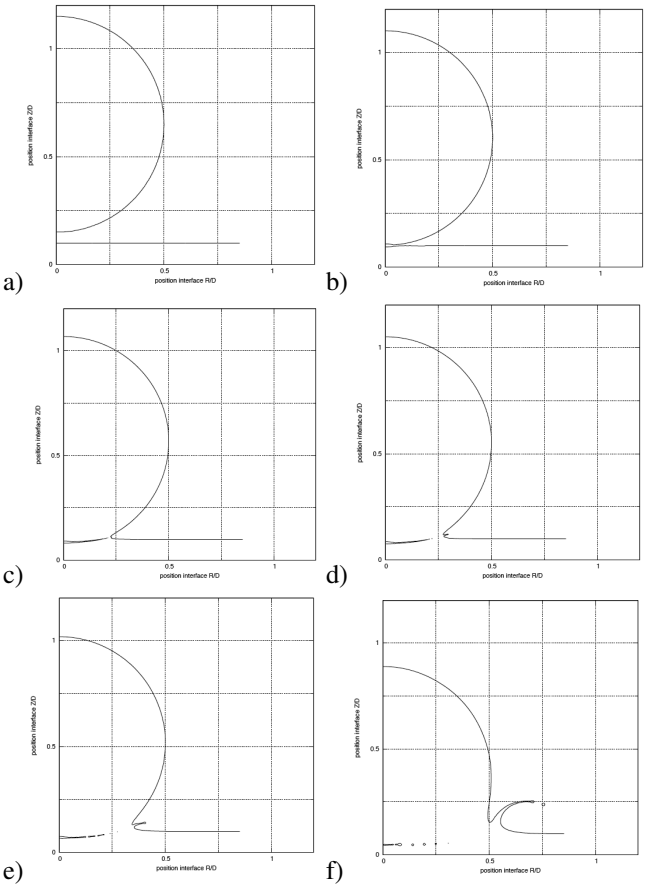

Figure 1: Snapshots of a drop of a water-like liquid impacting on a thin film of the same liquid. The surrounding fluid is air. The interface is drawn by the black solid line. The drop radius is 2 mm and the falling velocity is 4 m·s^{-1}. The liquid layer thickness is 0.4 mm. The simulation starts with $h = 0.267$ mm. The different interface profiles are shown at times $U{\cdot}t/D =$ a) 0.0017, b) 0.08, c) 0.1, d) 0.117, e) 0.15 and f) 0.28. The free fall time is such that $U \cdot t/D = 0.067$.

Finally, recent experiments of drop impacts on solid surface have shown that the air dynamics near impact could be crucial for the resulting dynamics (Xu et al. (2005)). There, the impact outcome changes dramatically from a gently spreading to splashing as the surrounding gas pressure is increasing. Theoretical approaches suggest that the viscous gas layer which dominates the dynamics near the onset of the impact could explain this striking effect (Korobkin et al. (2008); Mandre et al. (2009). In particular, they exhibit the formation of a finite time singularity for a simplified model of the impact: using the lubrication approximation in 2D for the cushioning air and neglecting the viscosity in the liquid and the surface tension, they observe for a parabolic shaped impact a finite time singularity as the dimple entrapped the bubble. At the closure point, both the pressure and the interface curvature diverge. The relation between such finite singularity in an idealized situation with the splashing transition is in debate and it is thus important to have a better understanding of the gas ejection dynamics as a drop approaches an other surface. It is in particular important to disentangle and characterize the different physical parameter involved in the impact. For instance, as shown by Mandre et al. (2009) the singularity is apparently disappearing when surface tension is incorporated and one would also expect the singularity to be suppressed when the viscosity of the liquid is considered. Many other aspects need to be investigated: are compressible effects crucial as simple dimensional analysis suggests? Does the singularity exist in 3D, and for a drop instead of a parabola impact, for any impact parameters?

Using numerical simulations of two-phase flows, we investigate in this paper the consequence of the bubble entrapment on the subsequent splashing dynamics for the case of drop impact on a thin liquid film. Both fluid (liquid and gas) will be considered incompressible and we will focus on the limit of large Weber and Reynolds numbers (defined precisely below) where splashing is usually present. In addition, we want to characterize how the bubble entrapment changes our former study Josserand and Zaleski (2003) where the splashing was understood as a complex interplay between mass conservation, viscous boundary layer and capillary retraction. In the next section, we briefly present the numerical method and the schematic problem performed here. In section 3 we show in details for an air-water case the bubble entrapment dynamics. Finally, we conclude in section 4 with a discussion on the influence of the liquid viscosity in the entrapment and splashing dynamics.

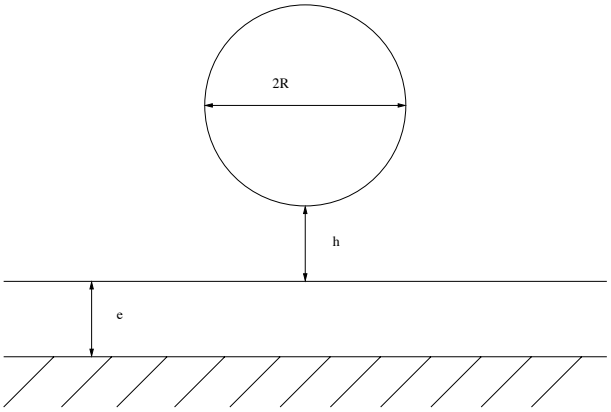

Figure 2: Sketch of the numerical simulation, a spherical drop of radius R and velocity U is considered at a distance h from a liquid film of thickness e.

2 Numerical method

We consider a drop of radius R (diameter $D = 2R$) impacting on a thin liquid film of thickness e with a velocity normal to the film interface U. Since we are interested in the air cushioning as the drop approach, the initial condition is taken as a spherical drop whose center is at distance $R + h$ from the film so that the initial air gap is h, as shown on figure (2).

Both fluid liquid and gas have densities ρ_l and ρ_g, and dynamical viscosities μ_l and μ_g. The problem can be characterized by the following dimensionless numbers:

$$\mathrm{Re} = \frac{2\rho_l U R}{\mu_l} \quad \text{and} \quad \mathrm{We} = \frac{2\rho_l U^2 R}{\sigma}$$

which are the liquid Reynolds number and the Weber number of the impact. These numbers compare the inertia with viscous effects and capillary forces for the liquid. Additional dimensionless numbers are also present in this problem corresponding to physical or geometrical ratios: the ratios between the gas and liquid densities and viscosities, ρ_g/ρ_l and μ_g/μ_l; the aspect ratios between the liquid film, the air gap and the drop e/R and h/R.

We have not taken here into account the gravity g and the gas compressibility. The influence of the gravity can be characterized by the Bond number $\mathrm{Bo} = gR/U^2$. For usual drop impact (water drop of millimeter radius, falling at a velocity of few meters per second, the Bond number is below 10^{-2} so that gravity can be safely neglected. For the gas compressibility, the question is more subtle: while the Mach numbers $\mathrm{Ma} = U/c_s$ where c_s is the speed of sound in each fluid are small in these typical impact dynamics, the compressibility of the gas can still become pertinent in the small region where the pressure diverge just before the contact as explained by Mandre et al. (2009). However, outside this small region the fluids can be considered incompressible and we will have this assumption further on by sake of simplicity.

We consider here axisymmetric flows: although we know that splashes generates high azimuthal instabilities responsible of secondary droplet break-up, this is a valid assumption for the small time after impacts. Since the bubble entrapment occurs in this regime, axisymetry is a good approximation to study this dynamics. The general 3D problem remains a great numerical challenge because of the large range of scales involved (Rieber and Frohn (1998); Gueyffier and Zaleski (1998)). Recent numerical results (Fuster et al. (2009)) show that we are close to be able to achieve realistic 3D numerical simulation. We however postpone the 3D study of drop impact to further works. Within this context, the general equation describing the problem is the two-phase Navier-Stokes equation that writes:

$$\rho(\frac{\partial \mathbf{u}}{\partial t} + \mathbf{u}\cdot\nabla\mathbf{u}) = -\nabla p + \mu\Delta\mathbf{u} + \sigma\kappa\delta_s\mathbf{n} \quad (1)$$

where $\mathbf{u} = (u, v)$ is the fluid velocity in the axisymmetric frame $(\mathbf{e}_r, \mathbf{e}_z)$, p is the pressure, and, ρ and μ the fluid densities and viscosities (different for the liquid and the gas). $\mathbf{n}$ denotes the normal to the interface and δ_s is the bidimensional delta function restricted to the interface. Thus in the liquid (gas) phase we have $\rho = \rho_l$ (ρ_g) and $\mu = \mu_l$ (μ_g). Additionnaly, the incompressibiity gives:

$$\mathrm{div}(\mathbf{u}) = 0.$$

The numerical simulation computes the flow evolution solving this incompressible two fluids equation (1, thanks to the GERRIS library that uses the Volume of Fluid (VOF) method on an adaptive grid allowing dynamical refinementPopinet (2003); Popinet, 2009). A characteristic function indicates the fraction of liquid phase in each grid cellBrackbill et al. (1992); Lafaurie et al. (1994). The viscosities and densities are constant in each phases while it is determined by the relative volume fraction of each phase for the cells crossed by the interface. The interface is then reconstructed using the piecewise linear interface calculation (PLIC) (Li (1995)). A quadtree structure in 2D (octree in 3D) allows for the dynamical mesh refinement. When refinement is needed, the mesh cell is divided into four equals square cells up to a maximum level n of refinement. The size of the minimal mesh cell is therefore $1/2^n$ times the size of the computational unit cell. Refinement criterion is based here on a mix of thr values of the density and the velocity gradients.

In the following calculations, where we will typically consider droplets of water-like liquid ($\rho_l = 1000$ kg $\cdot$ m^{-3}) of millimeter radius, we use a refinement level of 11 that allows for a resolution up to 0.1 μm.

3 Bubble entrapment

In this section, we will describe in details the impact of a water-like drop ($\rho_l = 1000$ kg $\cdot$ m^{-3}, $\mu_l = 0.016$ kg $\cdot$ m^{-1} $\cdot$ s^{-1}, 16 times the water viscosity) of $D = 4$ mm diameter, approaching a film of thickness $e = 0.4$ mm with a velocity $U = 4$ m $\cdot$ s^{-1} and surrounded by air gas ($\rho_g = 1$, $\mu_g = 10^{-5}$ kg $\cdot$ m^{-1} $\cdot$ s^{-1}, $\sigma = 0.072$ kg$\cdot$s^{-2}). The calculation starts when the drop is at a distance $h = 0.267$mm from the liquid film. The drop is taken initially spherical and we have choosen h high enough so that the liquid film is initially flat. For this configuration, the air Mach number is below 0.03 and the Bond number is below 10^{-3}. For these parameters, the Reynolds number of the liquid is 1000 and the Weber number is 889. Figure 1 shows that this impact leads to the entrapment of an air bubble and the formation of a thin jet followed by a corona splash.

We observe that as the drop approaches the liquid film, high pressures are created in the gas gap due to the cushioning of the air film. This high pressures are coming from the formation of a lubrication film of air that deforms the interface. Due to the lubrication layer structure, the pressure is higher below the drop center and a dimple forms so that the drop and the liquid film coalesce first at a finite radius. The formation of this dimple leading to a gas bubble entrapment was already described in different situations: using as well a full numerical simulation for the impact on a solid surface in axisymetric geometry (Mehdi-Nejad et al. (2003)); in planar 2D geometry for a model where the gas dynamics is solved in the lubrication approximation while the drop is replaced by the equivalent parabolic shape near the drop bottom , for impact on solid substrate and liquid layer on one hanf (Korobkin et al. (2008)), for impact on solid substrate accounting for the compressibility of the gas on the other hand (Mandre et al. (2009)). Figure 3 shows the maximal pressure in the fluid as a function of time for different Reynolds number.

As the impacting drop and the liquid film eventually connect, a high speed liquid jet emerges out of the small torus neck. Figure 4 shows snapshots of a zoom of the interface near the neck close to this colliding time. In the case studied here, we would like ti emphasize that the jet does not emerge immediately after the coalescence but that an other bubble torus is first entrapped between the vertically falling interface of the drop and the liquid film. This air torus can be clearly seen on figure 4d).

As questioning the influence of the refinement level

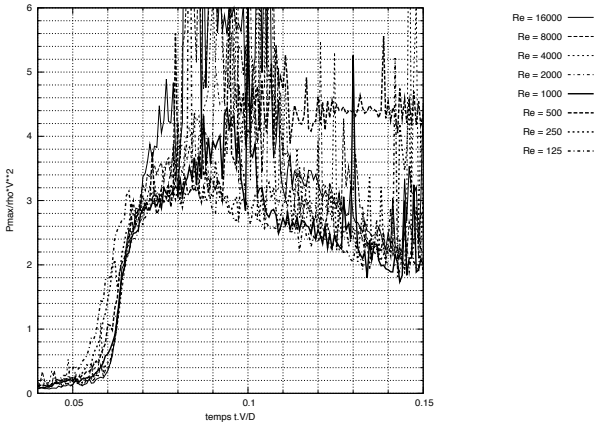

Figure 3: Maximum value of the pressure in the domain as function of time for different Reynolds number ranging from 125 to 16000. Beside the high fluctuations due to the high numerical fluctuations of the pressure at the interface at the lowest mesh size, a similar behavior is observed for the different Reynolds numbers.

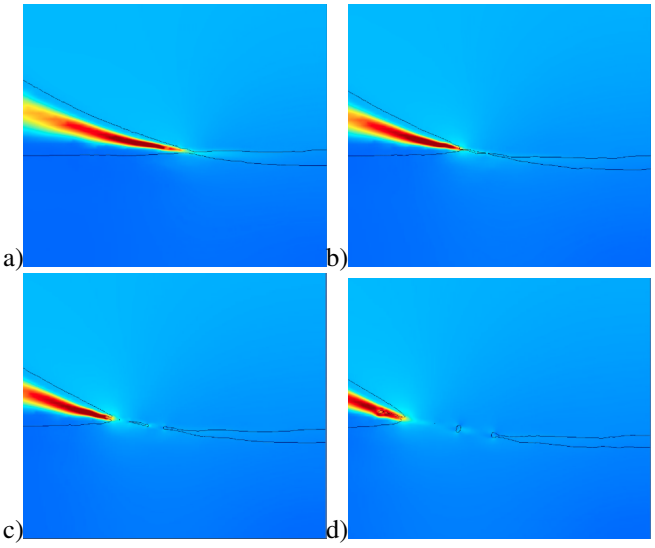

Figure 4: Zoom of the coalescence of the impacting drop on the liquid film near the radius at which the two interfaces first collapse. The colormap shows the norm of the velocity field.

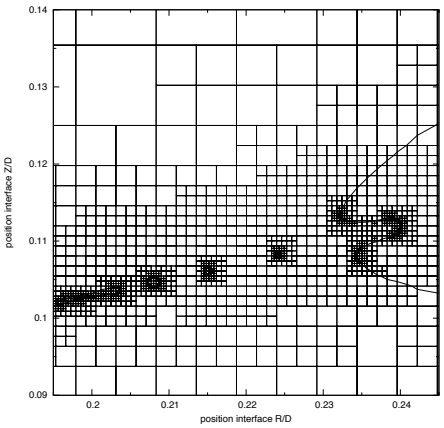

Figure 5: Exemple of the mesh-grid just after the emission of the jet.

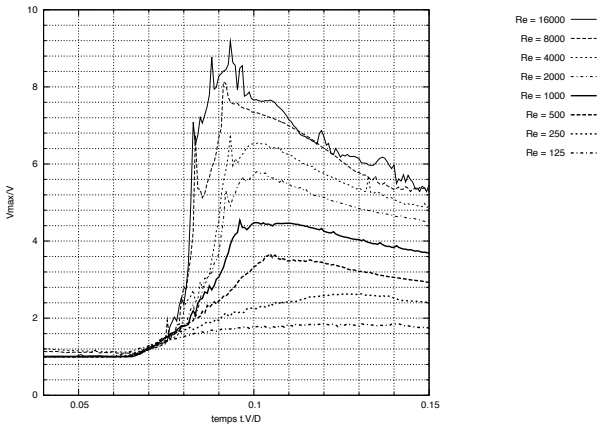

Figure 6: Evolution of the mamimum velocity in the liquid with time for different Reynolds numbers.

to the numerical results, we observe only small variations as the maximum level changes. Indeed, varying the maximum refinement level from 8 to 12 (it corresponds here to a minimum mesh size varying roughly from 2μm to 0.05μm), we observe that the variations in the position and the value of the maximum of the pressure and velocity fields are within the numerical fluctuations. However, most of the variations are concentrated near the coalescence time. In particular, when the refinement is lowered, we do not observe the secondary bubble entrapment seen in the level $n = 11$ simulation. This suggests that we might have successive entrapments of smaller and smaller (probably in a self similar sequence) air torus in a finite time as the maximal refinement would increase. We have not been able to see a third air bubble entrapment in the numerics up to $n = 12$ which was the highest available refinement level we have performed. As we will see below, an important feature to characterize the splashing is the thickness of the emitted jet at onset. It the very thin, is also affected by the level of refinement if it is not chosen big enough. Finally, we noticed that for our set of calculations, a refinement level above$n = 10$ was good enough to have almost mesh-independent results and most of our numerical simulations were done with $n_{max} = 11$. Figure 5 shows the mesh structure of the numerical simulation after the coalescence between the drop and the liquid layer, showing that the interface and the bubble are well resolved.

4 Influence of the liquid viscosity

The liquid viscosity is known to play a crucial role in the splashing dynamics: in fact, the liquid viscosity can control whether an impact will lead to a splash or a simple spread of the drop on the liquid film. In a previous work, two of us (C.J and S.Z) have explained how a subtle balance involving viscosity, surface tension and inertia/mass conservation was at the heart of the splashing dynamics. In a simplified model where no bubble entrapment was considered (and somehow the role of the surrounding gas neglected), we obtained in particular that the velocity of the splashing jet was scaling like $\sqrt{\mathrm{Re}}U$ as observed experimentally (Thoroddsen (2002)). How does this prediction change when the surrounding gas is considered, knowing that in experiment a bubble is entrapped *a priori*? Figure 6 shows the time evolution of the maximum velocity in the liquid for different Reynolds numbers. The velocity exhibits a high peak, particularly for high Reynolds numbers, which coincides with the connexion between the drop and the liquid layer. When the jet is formed, the maximum is precisely near the jet edge. We observe finally that the velocity peaks increases with the Reynolds numbers. The discussion of this dependance and the comparison with the predicted law of the simplified model will be discussed in further work.

Conclusions

The impact of a drop on a liquid layer is investigated numerically using a adaptive mesh refinement method that allows a consistent account of the gas layer down the drop. We observe the formation of a dimple and the entrapment of a gas bubble due to the high pressures created by the viscosity of the gas that has to be evacuated by the impact. Finally we discuss the discussion of this dynamics as the Reynolds number varies.

Acknowledgements

C.J. wants to acknowledge the A.N.R.

References

D. Bartolo, C. Josserand, and D. Bonn. Retraction dynamics of aqueous drops upon impact on nonwetting surfaces. *J. Fluid Mech*, 545:329–338, 2005.

D. Bartolo, C. Josserand, and D. Bonn. Singular jets and bubbles in drop impact. *Phys. Rev. Lett.*, 96:124501, 2006.

J.U. Brackbill, D. B. Kothe, and C. Zemach. A continuum method for modeling surface tension. *J. Comput. Phys.*, 100:335–354, 1992.

C. Clanet, C. Béguin, D. Richard, and D. Quéré. Maximal deformation of an impacting drop. *J. Fluid Mech*, 517:199–208, 2004.

Michel Coantic. Mass transfert across the ocean-air interface : small scale hydrodynamic and aerodynamic mechanisms. *PhysicoChemical Hydrodynamics*, 1:249–279, 1980.

D. Fuster, G. Agbaglah, C. Josserand, S. Popinet, and S. Zaleski. Numerical simulation of droplets, bubbles and waves: state of the art. *Fluid Dyn. Res.*, 41:065001, 2009.

D. Gueyffier and S. Zaleski. Formation de digitations lors de l'impact d'une goutte sur un film liquide. *C. R. Acad. Sci. IIb*, 326:839–844, 1998.

H.N. O guz and A. Prosperetti. Bubble entrainment by the impact of drops on liquid surfaces. *J. Fluid Mech.*, 219:143–179, 1990.

C. Josserand and S. Zaleski. Droplet splashing on a thin liquid film. *Phys. Fluids*, 15:1650, 2003.

C. Josserand, L. Lemoyne, R. Troeger, and S. Zaleski. Droplet impact on a dry surface: triggering the splash with a small obstacle. *J. Fluid Mech*, 524:47–56, 2005.

A.A. Korobkin, A.S. Ellis, and F.T. Smith. Trapping of air in impact between a body and shallow water. *J. Fluid Mech.*, 611:365–394, 2008.

B. Lafaurie, C. Nardone, R. Scardovelli, S. Zaleski, and G. Zanetti. Modelling merging and fragmentation in multiphase flows with SURFER. *J. Comput. Phys.*, 113: 134–147, 1994.

Jie Li. Calcul d'interface affine par morceaux (piecewise linear interface calculation). *C. R. Acad. Sci. Paris, série IIb, (Paris)*, 320:391–396, 1995.

Shreyas Mandre, Madhav Mani, and Michael P. Brenner. Precursors to splashing of liquid droplets on a solid surface. *Phys. Rev. Lett.*, 102:134502, 2009.

V. Mehdi-Nejad, J. Mostaghimi, and S. Chandra. Air bubble entrapment under an impacting droplet. *Phys. Fluids*, 15(1):173–183, 2003.

S. Popinet. Gerris flow solver-http://gfs.sourceforge.net/. URL `http://gfs.sourceforge.net/`.

S. Popinet. Gerris: a tree-based adaptive solver for the incompressible euler equations in complex geometries. *J. Comp. Phys.*, 190(2):572–600, 2003.

S. Popinet. An accurate adaptive solver for surface-tension-driven interfacial flows. *J. Comput. Phys.*, 228: 5838–5866, 2009.

A. Prosperetti and H.N. O guz. The impact of drops on liquid surfaces and the underwater noise of rain. *Annu. Rev. Fluid Mech.*, 25:577, 1993.

M. Rein. Phenomena of liquid drop impact on solid and liquid surfaces. *Fluid Dyn. Res.*, 12:61, 1993.

Y. Renardy, S. Popinet, L. Duchemin, M. Renardy, S. Zaleski, C. Josserand, M. Drumright-Clarke, D. Richard, C. Clanet, and D. Quéré. Pyramidal and toroidal water drops after impact on a solid surface. *J. Fluid Mech.*, 484:69–83, 2003.

M. Rieber and A. Frohn. Numerical simulation of splashing drops. Academic Press, 1998. Proceedings of ILASS98, Manchester.

R.D. Schroll, C. Josserand, S. Zaleski, and W.W. Zhang. Impact of a viscous liquid drop. *Phys. Rev. Lett.*, 104: 034504, 2010.

S. T. Thoroddsen, T. G. Etoh, and K. Takehara. Air entrapment under an impacting drop. *Journal of Fluid Mechanics*, 478:125–134, 2003.

S. T. Thoroddsen, T. G. Etoh, K. Takehara, N. Ootsuka, and A. Hatsuki. The air bubble entrapped under a drop impacting on a solid surface. *Journal of Fluid Mechanics*, 545:203–212, 2005.

S.T. Thoroddsen. The ejecta sheet generated by the impact of a drop. *J. Fluid Mech.*, 451:373, 2002.

L. Xu, W.W. Zhang, and S.R. Nagel. Drop splashing on a dry smooth surface. *Phys. Rev. Lett.*, 94:184505, 2005.

A.L. Yarin and D.A. Weiss. Impact of drops on solid surfaces: self-similar capillary waves, and splashing as a new type of kinematic discontinuity. *J. Fluid Mech.*, 283:141–173, 1995.